

3—34

Variational Specular Separation Using Color and Polarization

Dae-Woong Kim* Stephen Lin† Ki-Sang Hong* Heung-Yeung Shum†

*Pohang University of Science and Technology(POSTECH) ‡

†Microsoft Research, Asia

Abstract

In this paper, we propose a method that separates specular reflections from polarized color images. With line constraints in RGB color space and spatial domain information, we used a Variational energy minimization approach to restore diffuse reflections. With anisotropic smoothing, our method preserves the shape of textures and successfully separates specular reflections. Also, saturation of specular reflections is considered using a simple inpainting method.

1 Introduction

There are mainly two kinds of light reflection: specular and diffuse. Because of strong directional dependency, specular reflections present difficulties in many areas of computer vision algorithms such as shape from shading and photometric stereo.

To separate specular reflections, various algorithms have been developed. Brelstaff and Blake[1] addressed the problem of detecting specularities in gray level images with a Lambertian constraint. Klinker et al.[2] developed a color-based method from Shafer's dichromatic reflectance model[3]. Sato and Ikeuchi[4] achieved separation using color signatures generated by varying the illumination direction and Lin et al.[5] used a color histogram with multi-stereo images.

A polarization approach was introduced by Wolff and Boulton[6][7] where polarizing filters are used to effectively separate diffuse and specular reflections for areas with a constant Fresnel ratio. Nayar et al.[8] used polarization in conjunction with color information from a single view to separate reflection components. Their work relies on polarization for specular detection from dielectric materials and on color for separation of specular and diffuse reflection components using the dichromatic model. They showed that by varying the polarization filter, the color of the specular component can be determined independently for each image point resulting in a line subspace on which the diffuse vector must lie. Neighboring diffuse colors that satisfy these line constraints are used to compute the diffuse color vector for the point.

Extending previous work[8], we present a simple variational approach to separate specular reflections using color and polarization. We decomposed the color

space into two subspaces in each pixel: the specular line space and the diffuse plane space. The line space is parallel to the constraint line of polarization in each pixel, while the plane space represents a plane perpendicular to the specular direction. In specular line space, our energy functional smoothes anisotropically the spatial variation of specular components depending on boundary values, and the direction of the smoothing is controlled by gradient information in the diffuse plane space. As a constraint, anisotropic homogeneous smoothness of the separated specular reflections is employed in our energy functional and controlled by the gradient information of the polarization-varying specular intensity in the polarized images.

The narrow dynamic range of sensor and high incident angle can cause saturations with erroneous line constraints. To overcome this, a simple constrained Total Variation inpainting[9] method is applied during preprocessing. With this approach, our algorithm can deal with saturated specular images. In the energy minimization process following preprocessing, our method successfully separates specular reflections from the polarized images, which preserves overall textures and diffuse reflections.

2 Color and Polarization

For non-polarized incident light (which is typical), diffuse reflection is non-polarized, while specular reflection exhibits partial polarization. Because of partial polarization of specular reflections, the color intensity $I(\theta)$ of a pixel viewed through a polarizer with angle θ can be expressed as

$$I(\theta) = I_d + I_{sc} + I_{sv} \cos^2(\theta - \alpha), \quad (1)$$

where I_d is the diffuse intensity, I_{sc} is the polarization-constant specular intensity, I_{sv} is the polarization-varying specular intensity, and α is the phase angle determined by the projection of the surface normal onto the polarization filter plane.

The above equation predicts that a specular pixel as seen through different polarizer angles will have color readings that lie on a line in RGB space, as shown in Figure 1. This line extends toward the illumination direction from the underlying diffuse color, because the polarizer attenuates the partially polarized specular intensity but not the unpolarized diffuse component. For a user-defined threshold t , a pixel is considered to be specular region when

$$I_{max} - I_{min} = 2I_{sv} > t. \quad (2)$$

*Address: Dept. of E.E., POSTECH San 31, Hyoja-Dong, Pohang, Korea. E-mail: {dwkim,hongks}@postech.ac.kr

†Address: Microsoft Research, Beijing, China. E-mail: {stevelin,hshum}@microsoft.com

‡This work was performed while the first author was visiting Microsoft Research, Asia.

3 Separation of Specular and Diffuse Reflections

The specular constraint line in equation (1) can be represented as a parametric form $L(p)$ with the normalized line direction vector $[\alpha, \beta, \gamma]$ at each pixel (x, y) , as shown in Figure 1. I_{min} can be decomposed into two orthogonal vectors passing through the origin: I_{min}^l and I^g . The half line space I^l is the specular directional line parallel to $L(p)$ and reacts on polarizer, while I^g is a vector on the plane orthogonal to I^l and $L(p)$. It is noted that the vector I^g is a constant vector independent of the polarizer angle θ at each pixel.

To separate specular reflection from I_{min} , we have to locate $p_d(\geq 0)$ given by

$$p_d = |I_{min}^l| - |I_d^l| = |I_{min} - I_d|. \quad (3)$$

After I_d^l is determined, specular and diffuse reflections can be separated using a simple vector calculation. Therefore, to locate I_d^l , we only need to work on I^l space with the initial value I_{min}^l at each pixel.

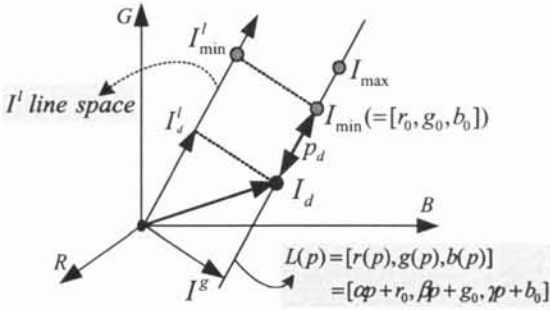


Figure 1: Decomposition of I_{min} at each pixel into I^g and I_{min}^l in RGB color space.

In the neighborhood, all decomposed I^g s lie on the same plane assuming a smooth illumination change, which results in parallel specular constraint lines. The approximated parallelism will be guaranteed by pre-processing with equation (7). If we define the plane as diffuse plane space as shown in Figure 2, I_{min}^l and I_d^l can be represented as a 1-dimensional height from the diffuse plane space and we can make a 2-dimensional image with heights for all pixel positions. Finally, assuming that all of the decomposed I^g s are constant, we only need to process 2-dimensional image I_{min}^l to separate diffuse reflection image.

Based on the decomposed specular line image I_{min}^l , we proposed a energy functional to be minimized:

$$E = \int_{\Omega} \nabla |I_d^l|^T D_l \nabla |I_d^l| + \lambda \nabla p_d^T D_p \nabla p_d, \quad (4)$$

$$D_l = v_l^T \begin{bmatrix} \mu & 0 \\ 0 & 1 \end{bmatrix} v_l, \mu = \frac{1}{1 + K|\nabla I^g|}, \quad (5)$$

$$D_p = v_p^T \begin{bmatrix} c & 0 \\ 0 & 1 - c \end{bmatrix} v_p, \quad (6)$$

where λ is the Lagrange multiplier, Ω is the detected specular region, and D_l, D_p are 2x2 constant matrices.

In equation (5), v_l is the eigenvector matrix of structure tensor from I^g and K is a constant which is similar to that of the anisotropic diffusion[11]. Because ∇I^g has information on texture variation independent of specular reflection, D_l guides the direction of the smoothing with v_l and adjusts the amount of smoothness with μ . Our model can be explained as an inpainting algorithm[9][10]. Image inpainting has previously been used to fill in missing areas in an image by extending boundary image information into the missing area. Our model fills the specular component of the boundary into the detected specular region. The matrix D_l controls the inpainting with v_l and μ . If $|\nabla I^g|$ is strong in some pixels, which means the strong diffuse texture in that region, then μ will place a barrier in that direction. Also, D_l becomes identity matrix in non-texture area resulting in isotropic smoothing.

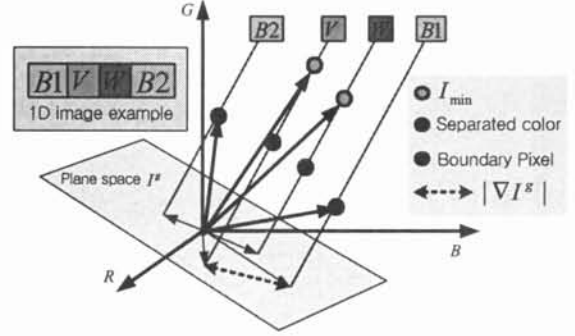


Figure 2: 1-dimensional I_{min}^l image example.

As a constraint term in the energy functional, the anisotropic shape information of the detected specular reflections is employed. Generally, specular reflections show an abrupt change in at most one direction and the direction of change can be approximated by the polarization-varying specular intensity I_{sv} . However, because the amount of change could not be known for lack of an exact I_{sc} , we introduced a homogeneous anisotropic smoothness shape prior to the detected specular reflections with the matrix D_p . v_p is the eigenvector matrix of structure tensor from I_{sv} , and c is a small constant.

Finally, our energy functional minimizes specular variation from the boundary to the edge direction of pure diffuse texture and separates the anisotropically smoothed specular reflections. Because of the anisotropic property of the process, our method can preserve the shape of textures independently of specular components.

4 Problem of Saturation

In our formulation and in previous work[8], the line is considered as an exact and strong constraint. This is a true assumption only if all intensities of the polarized images are not saturated, as in Figure 3(a). Pixel saturation resulting from such conditions as narrow dynamic range sensors or intense specular reflections can lead to an erroneous polarization line constraint, as shown in Figure 3(b). For example, if any component of R, G, and B is saturated, the direction of the line

equation deviates from the true line and the diffuse point in RGB space cannot be reached. If a blue component of I_{min} is extremely saturated, the line equation will be parallel to the RG plane, which results in no change of blue color.

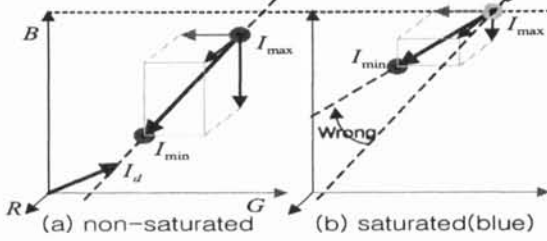


Figure 3: Saturation in a pixel

Because the direction of the constraint lines depend only on light illumination, they are almost parallel in their neighborhoods, which means the smooth change in the vector $[\alpha, \beta, \gamma]$. With this assumption, Total Variation inpainting method[9] with constraint is applied in the preprocessing:

$$E = \sum_{\Psi=\alpha,\beta,\gamma} \left[\int_{S \cup B} |\nabla \Psi| + \lambda_s \int_{\Omega \setminus S} (\Psi - \Psi_0)^2 \right],$$

subject to $\alpha^2 + \beta^2 + \gamma^2 = 1$, (7)

where $S(= \{x|x = 255, x \in \Omega\})$ represents the saturated region, λ_s is a positive constant, and Ψ_0 represents initial values in each component of $[\alpha, \beta, \gamma]$. In the non-saturated specular region $\Omega \setminus S$, the equation (7) denoises each α , β , and γ , which guarantees the approximated parallelism of the constraint lines. Due to the lack of polarization effect, constraint lines can be wrong in the boundary(B) of the detected specular region. For this reason, inpainting is performed in B as well as S , which results in smooth change of the line direction vector in the boundary. In other words, we used non-saturated line direction vectors in RGB space as a true information, and inpainted the information into S and B .

Figure 4 shows α, β, γ images before and after the inpainting preprocessing. we can notice the wrong values in saturated and boundary regions before inpainting. After inpainting, we restored α, β, γ depending on the non-saturated region. With this approach, our algorithm can deal with saturated specular images which successfully separates the specular reflection from the polarized images.

5 Implementation

With the Euler Lagrange equation (9) derived from (4), we used gradient descent algorithm with time step τ to obtain the solution:

$$|I_d^t|^{t+1} = |I_d^t|^t - \tau \frac{\partial E}{\partial t} \quad (8)$$

$$\frac{\partial E}{\partial t} = \nabla \cdot (D_t \nabla |I_d^t|) + \lambda \nabla \cdot (D_p \nabla p_d) = 0. \quad (9)$$

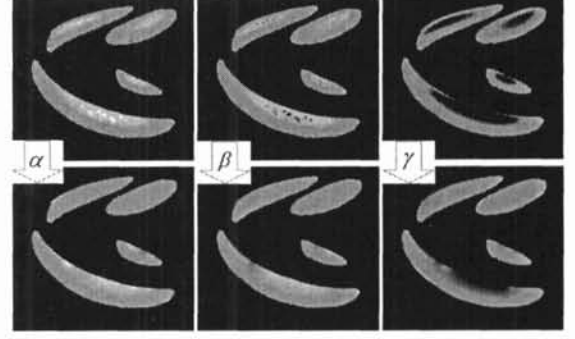


Figure 4: α, β, γ of Figure 6 represented by gray scale images (the first row: before inpainting, the second row: after inpainting).

Because the PDE (9) is a 2nd order derivative, it is easy to implement with a finite difference method and stable if τ is small. Also, the functional (7) is implemented by the same procedure as mentioned above, except the projection onto the space satisfying the constraint $\alpha^2 + \beta^2 + \gamma^2 = 1$ at the end of each iteration.

6 Experimental Results

In experiments, six images with equal polarizer angle differences are obtained from a digital camera equipped with a linear polarizer. From the experiment (Figure 5), specular variations are smoothed out (depending on the boundary values) in the flat region (red tomato), while the shape of stripe is preserved in the textured area (green pumpkin), as expected. Also, the separated specular reflections are very close to those in the I_{min} image (Figure 5(d)). However, in our implementation of Nayar's work[8], some pixels show noise-like results in the smooth region and pixels exist which are not processed for the lack of appropriate neighborhood pixels, as shown in Figure 5(e)(f).

With equation (1) and Fresnel ratio[7] (relating material property of the object and incident angle at each pixel), we made six polarization-simulated images in a graphical environment with single white light source, as shown Figure 6. Because G and B colors are saturated in some region, the separation fails without preprocessing. From the results, we observe that inpainting the line direction vectors in the saturated region works well if the non-saturated information is sufficient.

7 Conclusions

We proposed a method for separating specular reflections from polarized images based on energy minimization. Our method conserves the shape of texture and diffuse color in specular region by controlling the direction of smoothing with two constant matrices. We also considered pixel saturation and our method can deal with the case of inter-reflection if the change is smooth. Because our formulation is simple, it is easy to implement and can be extended with the other constraint.

It is a well known fact that the variation of diffuse reflections with illumination color can not be restored

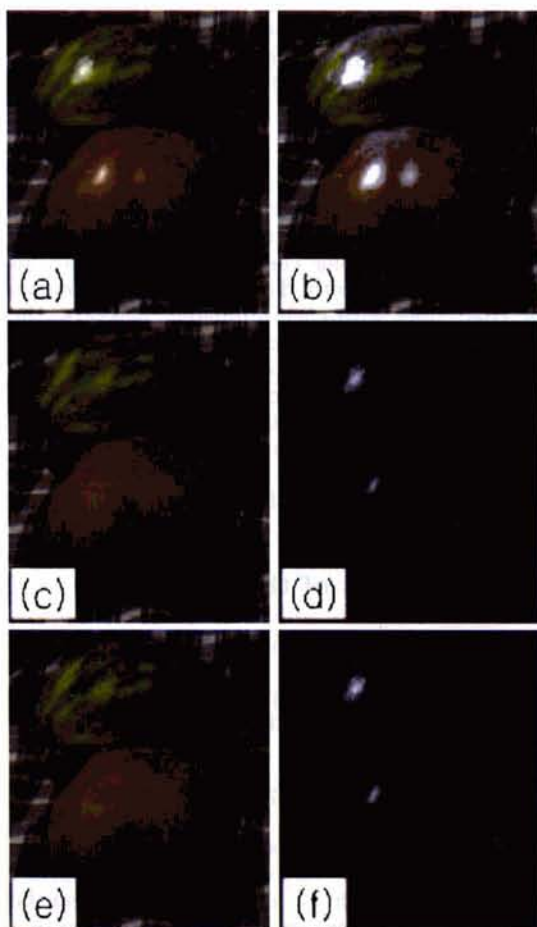


Figure 5: Experiment with real images. (a) I_{min} image. (b) detected specular region($t = 10$). (c)(d) separated diffuse(c) and specular(d) reflections($\lambda = 0.2$). (e)(f) separated results by Nayar's method[8].

in polarized images. This is also same limitation for our case. However, if there exists sufficient variation of diffuse reflections orthogonal to the illumination direction, our method can separate the specular reflections by controlling the direction of smoothing.

References

- [1] G. Brelstaff and A. Blake, "Detecting Specular Reflections using Lambertian Constraints," Proc. of Intl. Conf. on Computer Vision, pp.279-302, December 1992.
- [2] G. J. Klinker, S. A. Shafer, and T. Kanade, "The measurement of highlights in color images," International Journal of Computer Vision, Vol. 2, No. 1, pp.7-32, 1990.
- [3] S. Shafer, "Using color to separate reflection components," Color Research and Applications, Vol. 10, pp 210-218, 1985.
- [4] Y. Sato and K. Ikeuchi, "Temporal-Color Space Analysis of Reflection," Proc. of IEEE Conf. on Computer Vision and Pattern Recognition, pp.570-576, 1993.
- [5] S. Lin, Y. Li, S. B. Kang, X. Tong, and H. Y. Shum, "Diffuse-Specular Separation and Depth Recovery from Image Sequences," 7th European Conference on Computer Vision, pp. 210(Part III), 2002.
- [6] L. B. Wolff and T. E. Boult, "Constraining Object Features using a Polarization Reflectance Model," IEEE Trans. on Pattern Analysis and Machine Intelligence, Vol. 13, No. 7, pp.635-657, July 1991.
- [7] L. B. Wolff, "Using polarization to separate reflection components," In Proc. of IEEE Conf. on Computer Vision and Pattern Recognition, pp.363-369, 1989.
- [8] S. K. Nayar, X. Fang, and T. E. Boult, "Removal of specularities using color and polarization," In Proc. IEEE Conf. Computer Vision and Pattern Recognition., 1993.
- [9] T. Chan and J. Shen, "Mathematical models for local non-texture inpainting," March 2000 [SIAM J. Appl. Math, 62(3), pp.1019-1043, 2001].
- [10] M. Bertalmio, G. Sapiro, C. Ballester and V. Caselles, "Image inpainting," Computer Graphics, SIGGRAPH 2000, July 2000.
- [11] Bart M. ter Haar Romeny, "Geometry-Driven Diffusion in Computer Vision," Kluwer Academic Publishers, 1994.

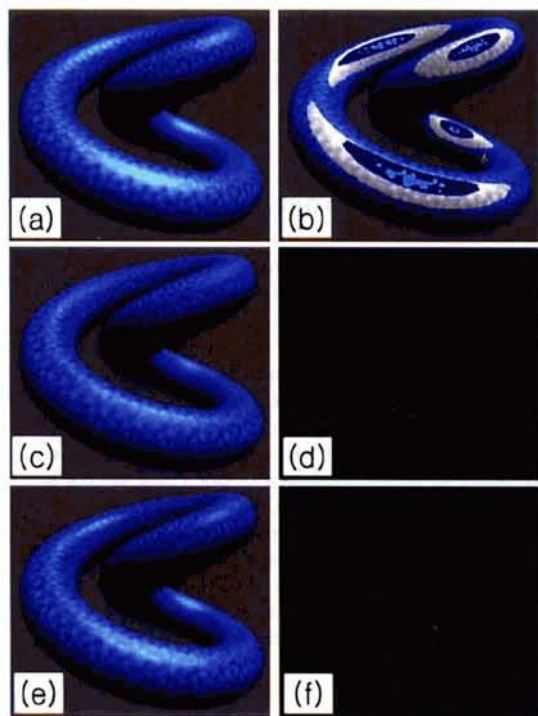


Figure 6: Experiment with simulated images. (a) I_{min} image. (b) detected specular region($t = 4$), Ω :gray scaled, S :colored. (c)(d) separated diffuse(c) and specular(d) reflections($\lambda = 0.4$) (e)(f) separated results without the preprocessing.